Institute of Sound and Vibration Research

The Fourier Transformed Stationary and Moving Dynamic Flexibility Matrices of a Layered Ground

X. Sheng, C.J.C. Jones and M. Petyt

ISVR Technical Memorandum No 837

March 1999

University of Southampton

SCIENTIFIC PUBLICATIONS BY THE ISVR

Technical Reports are published to promote timely dissemination of research results by ISVR personnel. This medium permits more detailed presentation than is usually acceptable for scientific journals. Responsibility for both the content and any opinions expressed rests entirely with the author(s).

Technical Memoranda are produced to enable the early or preliminary release of information by ISVR personnel where such release is deemed to the appropriate. Information contained in these memoranda may be incomplete, or form part of a continuing programme; this should be borne in mind when using or quoting from these documents.

Contract Reports are produced to record the results of scientific work carried out for sponsors, under contract. The ISVR treats these reports as confidential to sponsors and does not make them available for general circulation. Individual sponsors may, however, authorize subsequent release of the material.

UNIVERSITY OF SOUTHAMPTON

INSTITUTE OF SOUND AND VIBRATION RESEARCH

DYNAMICS GROUP

The Fourier Transformed Stationary and Moving Dynamic Flexibility Matrices of a Layered Ground

by

X. Sheng, C.J.C. Jones and M. Petyt

ISVR Technical Memorandum No. 837

March 1999

Authorized for issue by
Dr. M.J. Brennan
Group Chairman

The Fourier transformed stationary and moving dynamic flexibility matrices of a Layered Ground

Xiaozhen Sheng
Civil Engineering Department, East China Jiaotong University
Nanchang, Jiangxi, 330013, P. R. China
AND
C. J. C. Jones, M. Petyt
I.S.V.R., University of Southampton, Southampton, SO17 1BJ, England

SUMMARY

In this paper, a more efficient and analytical method to calculate the Fourier transformed stationary and moving dynamic flexibility matrices of a layered ground is proposed. These flexibility matrices will lead to significant advances in the investigation of a viariety of radiation, scattering and interaction problems associated with stationary and moving disturbances in a layered ground. The properties of these matrices are discussed and the reciprocity relations which are well known in the stationary case are extended to the moving case.

The Fourier transformed stationary and moving dynamic flexibility matrices of a layered ground

1 Introduction

For many applications, the relationships between the Fourier transfromed displacemnets and stresses at both sides of a layer in a layered ground subject to stationary (Loads act at a fixed point) or moving (Loads move in a fixed direction) harmonic loads are necessary. In the stationary case, several forms of these relationships are available. One relates the displacements and stresses at one side of the layer to the corresponding variables at the other side of the layer. This formulation is generally known as Haskell-Thomson technique (Thomson 1950, Haskell 1953) in the fields of soil dynamics, earthquake engineering and geophysics. An alternative is to relate the displacements at both sides of the layer to the tractions at both sides of the layer, resulting in direct or exact dynamic stiffness matrix (Kausel and Roesset 1981, Wolf 1985). The two aforementioned methods all use the analytical solution of the wave equation in a displacement formulation. When, alternatively, the exact solution of the wave equation is maintained in the horizontal direction, while a polynomial expansion is used in the vertical direction, a so-called thin layer formulation is obtained (Lysmer and Waas 1972, Waas 1972, Kausel and Peek 1982, Tassoulas and Kausel 1983, Kausel 1986). To avoid computational difficulties due to the exponential terms for large thickness of the layers in the dynamic stiffness matrix, the ground layers are divided into thin sub-layers and a global dynamic stiffness matrix constructed from the sub-layers's dynamic stiffness matrices is used (Jones and Petyt 1997, 1998), which increases greatly the scale of the problem.

In the moving case, making use of an exact factorization of the displacement and stress fields in terms of generlised transmission and reflection coefficients, Barros and Luco (1994) propose a procedure to obtain the steady state displacements and stresses within a layered ground generated by a buried or surface load moving with constant speed parallel to the ground surface. This procedure seems being too complicated.

Rather than use either the exact or discretized dynamic stiffness matrix techniques, it has been found by the present authors that improved computational efficiency can be achieved by using the dynamic flexibility matrix approach (similar to Haskell-Thomson technique) in which all the matrices being manipulated are of order less than or equal to 6. The definition of dynamic flexibility matrix in the stationary case is given in Section 2. The derivation of this flexility matrix for a three-dimensional ground layer is described for a Cartesian co-ordinate system in Section 3. With some mathematical treatment and making use of some properties of the matrix described in Section 4, numerical difficulties that occur in a number of previous work are avoided, and explicit analytical expressions of the formulae are obtained. In Section 5, the formulae developed for the stationary case are extended to include the case when harmonic loads move uniformly along a direction parallel to the ground surface, and reciprocity relations are then proved. And lastly, Section 6 gives example calculations for comparsion with other methods.

The ground consists of a number, n, of parallel layers of different materials. The nth layer overlies a half space or a rigid foundation, which is identified as 'layer' number $(n+1)$. For the jth layer the material constants are: elastic modulus, E_j, Poisson ratio, ν_j; density, ρ_j; loss factor, η_j and layer thickness, h_j. If the $(n+1)$th layer is a half space, its material constants are E_{n+1}, ν_{n+1}, ρ_{n+1} and η_{n+1}. In the coordinate system $Oxyz$, the plane Oxy stands for the ground surface, and z-axle is downward in the ground.

2 Definition of dynamic flexibility matrix

The steady state vibrational displacement amplitudes of the point $R(x,y)$ on the top side of the l_Rth ($1 \le l_R \le n+1$)layer of the ground in x,y,z directions, due to a unit harmonic load $e^{i\omega t}$, where $i = \sqrt{-1}, \omega$ is angular frequency, acting at the point $P(0,0)$ on the top side of the l_Pth ($1 \le l_P \le n+1$) layer in the x direction, are denoted by $Q_{11}(x,y)$, $Q_{21}(x,y)$, $Q_{31}(x,y)$, respectively; when the unit harmonic load acts at P in the y direction, the amplitudes are denoted by $Q_{12}(x,y)$,$Q_{22}(x,y)$,$Q_{32}(x,y)$; and $Q_{13}(x,y)$, $Q_{23}(x,y)$, $Q_{33}(x,y)$ when the unit load is in z direction. A matrix, $[Q(x,y)]$, can be defined as

$$[Q(x,y)] = \begin{bmatrix} Q_{11}(x,y) & Q_{12}(x,y) & Q_{13}(x,y) \\ Q_{21}(x,y) & Q_{22}(x,y) & Q_{23}(x,y) \\ Q_{31}(x,y) & Q_{32}(x,y) & Q_{33}(x,y) \end{bmatrix} \tag{1}$$

This is called *the stationary dynamic flexibility matrix of l_R to l_P* (meaning that, the unit harmonic loads act at the origin point of the top plane of l_Pth layer and the displacements are for the top side of l_Rth layer), or simply, *stationary dynamic flexibility matrix*. In general the Q's are complex, and alternatively called displacement Green's functions.

Now suppose that, in the top side of l_Pth layer, the harmonic load distributions $p_x(x,y)e^{i\omega t}, p_y(x,y)e^{i\omega t}, p_z(x,y)e^{i\omega t}$ act in x, y, z directions respectively. The total steady state vibration amplitudes of the point $R(x,y)$ in x, y, z directions, denoted by $u_{l_R 0}(x,y), \upsilon_{l_R 0}(x,y), w_{l_R 0}(x,y)$, are

$$\begin{Bmatrix} u_{l_R0}(x,y) \\ \upsilon_{l_R0}(x,y) \\ w_{l_R0}(x,y) \end{Bmatrix} = \begin{Bmatrix} u_{l_R0} \\ \upsilon_{l_R0} \\ w_{l_R0} \end{Bmatrix} = \int_{-\infty}^{\infty}\int_{-\infty}^{\infty} [Q(x-r, y-s)] \begin{Bmatrix} p_x(r,s) \\ p_y(r,s) \\ p_z(r,s) \end{Bmatrix} drds \tag{2}$$

Equation (2) is a convolution integration. Using the Fourier transform pairs

$$\left.\begin{aligned} &\tilde{f}(\beta) = \int_{-\infty}^{\infty} f(x)e^{-i\beta x}dx, \qquad f(x) = \tfrac{1}{2\pi}\int_{-\infty}^{\infty} \tilde{f}(\beta)e^{i\beta x}d\beta \\ &\tilde{f}(\beta,\gamma) = \int_{-\infty}^{\infty}\int_{-\infty}^{\infty} f(x,y)e^{-i(\beta x+\gamma y)}dxdy, f(x,y) = \tfrac{1}{4\pi^2}\int_{-\infty}^{\infty}\int_{-\infty}^{\infty} \tilde{f}(\beta,\gamma)e^{i(\beta x+\gamma y)}d\beta d\gamma \end{aligned}\right\} \tag{3}$$

to transform equation (2) into the domain of the wavenumbers β in the x direction and γ in the y direction, yields

$$\begin{Bmatrix} \tilde{u}_{l_R0}(\beta,\gamma) \\ \tilde{\upsilon}_{l_R0}(\beta,\gamma) \\ \tilde{w}_{l_R0}(\beta,\gamma) \end{Bmatrix} = [\tilde{Q}(\beta,\gamma)] \begin{Bmatrix} \tilde{p}_x(\beta,\gamma) \\ \tilde{p}_y(\beta,\gamma) \\ \tilde{p}_z(\beta,\gamma) \end{Bmatrix} = [\tilde{Q}(\beta,\gamma)]\{\tilde{p}(\beta,\gamma)\} \tag{4}$$

where, $\tilde{u}_{l_R0}(\beta,\gamma)$ stands for the Fourier transform of $u_{l_R0}(x,y)$, etc. The matrix $[\tilde{Q}(\beta,\gamma)]$ is called the *Fourier transformed stationary dynamic flexibility matrix of l_R to l_P*, or simply the *Fourier tranformed stationary dynamic flexibility matrix.* The derivation of an exact expression for this matrix is dealt with below in Section 3.

3 Derivation of the Fourier transformed dynamic flexibility matrix

3.1 Analysis for a single (jth) layer (j=1,2,...,n)

The steady-state displacements at the point (x, y, z) (where $z \in (0,h_j)$) are denoted by $u_j(x,y,z)e^{i\omega t}, \upsilon_j(x,y,z)e^{i\omega t}, w_j(x,y,z)e^{i\omega t}$, where $u_j(x,y,z)$ and etc. are generally complex numbers and their Fourier transforms are denoted by $\tilde{u}_j(\beta,\gamma,z), \tilde{\upsilon}_j(\beta,\gamma,z), \tilde{w}_j(\beta,\gamma,z)$. The three components of stresses in x, y, z directions on the top of the jth layer are $\tau_{xzj}(x,y,0)e^{i\omega t}, \tau_{yzj}(x,y,0)e^{i\omega t}, \tau_{zzj}(x,y,0)e^{i\omega t}$, and those at the bottom are $\tau_{xzj}(x,y,h_j)e^{i\omega t}, \tau_{yzj}(x,y,h_j)e^{i\omega t}, \tau_{zzj}(x,y,h_j)e^{i\omega t}$. The Fourier transforms of the stress amplititutes are denoted by

$\tilde{\tau}_{xzj}(\beta,\gamma,0), \tilde{\tau}_{yzj}(\beta,\gamma,0), \tilde{\tau}_{zzj}(\beta,\gamma,0), \tilde{\tau}_{xzj}(\beta,\gamma,h_j), \tilde{\tau}_{yzj}(\beta,\gamma,h_j), \tilde{\tau}_{zzj}(\beta,\gamma,h_j)$

Put

$$\left.\begin{aligned}
&\{\tilde{u}\}_{j0} = (\tilde{u}_j(\beta,\gamma,0), \tilde{\upsilon}_j(\beta,\gamma,0), \tilde{w}_j(\beta,\gamma,0))^T \\
&\{\tilde{\tau}\}_{j0} = (\tilde{\tau}_{xzj}(\beta,\gamma,0), \tilde{\tau}_{yzj}(\beta,\gamma,0), \tilde{\tau}_{zzj}(\beta,\gamma,0))^T \\
&\{\tilde{S}\}_{j0} = \begin{Bmatrix} \{\tilde{u}\}_{j0} \\ \{\tilde{\tau}\}_{j0} \end{Bmatrix}
\end{aligned}\right\} \tag{5}$$

$$\left.\begin{aligned}
&\{\tilde{u}\}_{j1} = (\tilde{u}_j(\beta,\gamma,h_j), \tilde{\upsilon}_j(\beta,\gamma,h_j), \tilde{w}_j(\beta,\gamma,h_j))^T \\
&\{\tilde{\tau}\}_{j1} = (\tilde{\tau}_{xzj}(\beta,\gamma,h_j), \tilde{\tau}_{yzj}(\beta,\gamma,h_j), \tilde{\tau}_{zzj}(\beta,\gamma,h_j))^T \\
&\{\tilde{S}\}_{j1} = \begin{Bmatrix} \{\tilde{u}\}_{j1} \\ \{\tilde{\tau}\}_{j1} \end{Bmatrix}
\end{aligned}\right\} \tag{6}$$

where $\{\tilde{S}\}_{j0}$ is the (Fourier transformed) displacement and stress vector for the top interface of the jth layer, and $\{\tilde{S}\}_{j1}$ for the bottom. One can derive the relation between $\{\tilde{S}\}_{j0}$ and $\{\tilde{S}\}_{j1}$.

Because all displacements are harmonic, the Lamé equation for jth layer can be written as

$$\left.\begin{aligned}
&(\lambda_j+\mu_j)\tfrac{\partial\Delta_j}{\partial x}+\mu_j\nabla^2 u_j=-\rho_j\omega^2 u_j \\
&(\lambda_j+\mu_j)\tfrac{\partial\Delta_j}{\partial y}+\mu_j\nabla^2 \upsilon_j=-\rho_j\omega^2 \upsilon_j \\
&(\lambda_j+\mu_j)\tfrac{\partial\Delta_j}{\partial z}+\mu_j\nabla^2 w_j=-\rho_j\omega^2 w_j \\
&\Delta_j=\tfrac{\partial u_j}{\partial x}+\tfrac{\partial \upsilon_j}{\partial y}+\tfrac{\partial w_j}{\partial z} \\
&\lambda_j=\tfrac{\nu_j E_j(1+i\eta_j\,\mathrm{sgn}(\omega))}{(1+\nu_j)(1-2\nu_j)} \\
&\mu_j=\tfrac{E_j(1+i\eta_j\,\mathrm{sgn}(\omega))}{2(1+\nu_j)}
\end{aligned}\right\} \quad (j=1,2,..,n) \tag{7}$$

Fourier transforming equation (7) gives

$$\tilde{\Delta}_j = i\beta\tilde{u}_j + i\gamma\tilde{\upsilon}_j + \tfrac{d\tilde{w}_j}{dz} \tag{8}$$

$$\left.\begin{aligned}
&(\lambda_j+\mu_j)i\beta\tilde{\Delta}_j+\mu_j[\tfrac{d^2\tilde{u}_j}{dz^2}-(\beta^2+\gamma^2-\tfrac{\omega^2\rho_j}{\mu_j})\tilde{u}_j]=0 \\
&(\lambda_j+\mu_j)i\gamma\tilde{\Delta}_j+\mu_j[\tfrac{d^2\tilde{\upsilon}_j}{dz^2}-(\beta^2+\gamma^2-\tfrac{\omega^2\rho_j}{\mu_j})\tilde{\upsilon}_j]=0 \\
&(\lambda_j+\mu_j)\tfrac{d\tilde{\Delta}_j}{dz}+\mu_j[\tfrac{d^2\tilde{w}_j}{dz^2}-(\beta^2+\gamma^2-\tfrac{\omega^2\rho_j}{\mu_j})\tilde{w}_j]=0
\end{aligned}\right\} \quad (j=1,2,\dots,n+1) \tag{9}$$

From equations (8) and (9) results in

$$\frac{d^2\tilde{\Delta}_j}{dz^2} - (\beta^2 + \gamma^2 - \zeta_{j1}^2)\tilde{\Delta}_j = 0 \tag{10}$$

where, if the compression and shear wave speeds of the *j*th layer are denoted by

$$c_{j1} = \sqrt{\frac{\lambda_j + 2\mu_j}{\rho_j}}, \quad c_{j2} = \sqrt{\mu_j / \rho_j} \tag{11}$$

respectively, and

$$\zeta_{j1} = \omega / c_{j1}, \zeta_{j2} = \omega / c_{j2} \tag{12}$$

are the compression wave number and shear wave number.

The general solution to equation (10) for $\tilde{\Delta}_j$, and then to equation (9) for $\tilde{u}_j, \tilde{\upsilon}_j$ and $\tilde{w}_j$ can be obtained by the characteristic root method of solving ordinary differential equations. Substituting the solutions to equations (9) and (10) into the Fourier transform of the stress-strain relation of the material, i.e.

$$\left.\begin{aligned} \tilde{\tau}_{xzj} &= \mu_j(i\beta\tilde{w}_j + d\tilde{u}_j / dz) \\ \tilde{\tau}_{yzj} &= \mu_j(i\gamma\tilde{w}_j + d\tilde{\upsilon}_j / dz) \\ \tilde{\tau}_{zzj} &= (\lambda_j\tilde{\Delta}_j + 2\mu_j d\tilde{w}_j / dz) \end{aligned}\right\} \tag{13}$$

gives $\tilde{\tau}_{xzj}$ and etc. All the results may be expressed in matrix forms as

$$\{\tilde{S}\}_{j0} = [A]_{j0}\{b\}_j \tag{14}$$

$$\{\tilde{S}\}_{j1} = e^{\alpha_{j1}h_j}[A]_{j1}\{b\}_j \tag{15}$$

where $\{b\}_j \in C^6$ are integration constants, and $[A]_{j0}$, $[A]_{j1}$ are 6x6 matrices dependent on wave numbers β and γ, frequency ω and material parameters. When $\beta=0$, the detailed expressions for $[A]_{j0}$ and $[A]_{j1}$are given in the Appendix, with

$$\alpha_{j1}^2 = \beta^2 + \gamma^2 - \zeta_{j1}^2, \; \alpha_{j2}^2 = \beta^2 + \gamma^2 - \zeta_{j2}^2 \tag{16}$$

The combination of equations (14) and (15) links the Fourier transformed displacements and the stresses at the bottom of the layer with those at the top:

$$\{\tilde{S}\}_{j1} = e^{\alpha_{j1}h_j}[A]_{j1}[A]_{j0}^{-1}\{\tilde{S}\}_{j0} \tag{17}$$

3.2 For the half space ($n+1$th layer, if it's not rigid)

Putting

$$\left.\begin{aligned} \{\tilde{u}\}_{n+1,0} &= (\tilde{u}_{n+1}(\beta,\gamma,0), \tilde{\upsilon}_{n+1}(\beta,\gamma,0), \tilde{w}_{n+1}(\beta,\gamma,0))^T \\ \{\tilde{\tau}\}_{n+1,0} &= (\tilde{\tau}_{xz,n+1}(\beta,\gamma,0), \tilde{\tau}_{yz,n+1}(\beta,\gamma,0), \tilde{\tau}_{zz,n+1}(\beta,\gamma,0))^T \end{aligned}\right\}$$

similar to equation (17), it can be shown that

$$\{\tilde{u}\}_{n+1,0} = [R][S]^{-1}\{\tilde{\tau}\}_{n+1,0} \tag{18}$$

where $[R]$ and $[S]$ are 3x3 matrices, the elements of which are shown in Appendix.

3.3 For the layered ground

The continuity of displacements and the balance of stresses at each interface of the layers imply that $\{\tilde{S}\}_{j1} = \{\tilde{S}\}_{j+1,0} (j=1,2,\ldots,n, j \neq l_P - 1), \{\tilde{S}\}_{l_P-1,1} = \{\tilde{S}\}_{l_P 0} + \{\tilde{S}\}^P$, where $\{\tilde{S}\}^P = (0,0,0,\tilde{p}_x,\tilde{p}_y,\tilde{p}_z)^T$. From equation (17) yields

$$\begin{aligned}
\{\tilde{S}\}_{n1} &= e^{\sum_{j=l_P}^{n}\alpha_{j1}h_j}[A]_{n1}[A]_{n0}^{-1}[A]_{n-1,1}[A]_{n-1,0}^{-1}\cdots[A]_{l_P 1}[A]_{l_P 0}^{-1}\{\tilde{S}\}_{l_P 0} \\
&= e^{\sum_{j=l_P}^{n}\alpha_{j1}h_j}[A]_{n1}[A]_{n0}^{-1}[A]_{n-1,1}[A]_{n-1,0}^{-1}\cdots[A]_{l_P 1}[A]_{l_P 0}^{-1}(\{\tilde{S}\}_{l_P-1,1} - \{\tilde{S}\}^P) \\
&= e^{\sum_{j=1}^{n}\alpha_{j1}h_j}[A]_{n1}[A]_{n0}^{-1}[A]_{n-1,1}[A]_{n-1,0}^{-1}\cdots[A]_{11}[A]_{10}^{-1}\{\tilde{S}\}_{10} - \\
&\quad - e^{\sum_{j=l_P}^{n}\alpha_{j1}h_j}[A]_{n1}[A]_{n0}^{-1}[A]_{n-1,1}[A]_{n-1,0}^{-1}\cdots[A]_{l_P 1}[A]_{l_P 0}^{-1}\{\tilde{S}\}^P
\end{aligned}$$

Putting

$$[T] = \begin{bmatrix}[T]_{11} & [T]_{12} \\ [T]_{21} & [T]_{22}\end{bmatrix} = [A]_{n1}[A]_{n0}^{-1}[A]_{n-1,1}[A]_{n-1,0}^{-1}\cdots[A]_{11}[A]_{10}^{-1} \tag{19}$$

$$[F] = \begin{bmatrix}[F]_{11} & [F]_{12} \\ [F]_{21} & [F]_{22}\end{bmatrix} = [A]_{n1}[A]_{n0}^{-1}[A]_{n-1,1}[A]_{n-1,0}^{-1}\cdots[A]_{l_P 1}[A]_{l_P 0}^{-1} \tag{20}$$

where $[T]_{11}$, $[F]_{11}$ and etc. are 3x3 matrices, one get

$$\begin{Bmatrix}\{\tilde{u}\}_{n1} \\ \{\tilde{\tau}\}_{n1}\end{Bmatrix} = e^{\sum_{j=1}^{n}\alpha_{j1}h_j}\begin{bmatrix}[T]_{11} & [T]_{12} \\ [T]_{21} & [T]_{22}\end{bmatrix}\begin{Bmatrix}\{\tilde{u}\}_{10} \\ \{\tilde{\tau}\}_{10}\end{Bmatrix} - e^{\sum_{j=l_P}^{n}\alpha_{j1}h_j}\begin{bmatrix}[F]_{11} & [F]_{12} \\ [F]_{21} & [F]_{22}\end{bmatrix}\begin{Bmatrix}0 \\ \{\tilde{p}\}\end{Bmatrix} \tag{21}$$

If the n+1th layer is a half space, then $\{\tilde{u}\}_{n+1,0} = \{\tilde{u}\}_{n1}, \{\tilde{\tau}\}_{n+1,0} = \{\tilde{\tau}\}_{n1}$. From equations (18) and (21) and noticing $\{\tilde{\tau}\}_{10} = 0$, yields

$$\{\tilde{u}\}_{10} = -e^{-\sum_{j=1}^{l_P-1}\alpha_{j1}h_j}([R][S]^{-1}[T]_{21} - [T]_{11})^{-1}([F]_{12} - [R][S]^{-1}[F]_{22})\{\tilde{p}\} \tag{22}$$

If the n+1th layer is a rigid foundation, meaning that $\{\tilde{u}\}_{n+1,0} = \{\tilde{u}\}_{n1} = 0$, from equation (21) yields

$$\{\tilde{u}\}_{10} = e^{-\sum_{j=1}^{l_P-1}\alpha_{j1}h_j}[T]_{11}^{-1}[F]_{12}\{\tilde{p}\} \tag{23}$$

Equations (22) and (23) are the relationships between the Fourier transformed displacement vector on the ground surface and the Fourier transformed load vector on the top side of l_Pth layer. If $l_P=1$ and the ground is just a half space (in this case, n=0), equation (18) applies.

3.4 The Fourier transformed dynamic flexibility matrix

For the responses of the top surface of the l_Rth layer, three cases should be accounted for:

(1) When $l_R<l_P$

Equation (17) yields

$$\{\tilde{S}\}_{l_R0} = e^{\sum_{j=1}^{l_R-1}\alpha_{j1}h_j}[A]_{l_R-1,1}[A]_{l_R-1,0}^{-1}\cdots[A]_{11}[A]_{10}^{-1}\{\tilde{S}\}_{10}$$

Putting

$$[G]=\begin{bmatrix}[G]_{11} & [G]_{12}\\ [G]_{21} & [G]_{22}\end{bmatrix}=[A]_{l_R-1,1}[A]_{l_R-1,0}^{-1}\cdots[A]_{11}[A]_{10}^{-1} \tag{24}$$

where $[G]_{11}$ and ect. are 3x3 matrices. Equation (22) then yields

$$\{\tilde{u}\}_{l_R0} = -e^{-\sum_{j=l_R}^{l_P-1}\alpha_{j1}h_j}[G]_{11}([R][S]^{-1}[T]_{21}-[T]_{11})^{-1}([F]_{12}-[R][S]^{-1}[F]_{22})\{\tilde{p}\} \tag{25}$$

(2) When $l_R>l_P$

$$\{\tilde{S}\}_{l_R0} = e^{\sum_{j=1}^{l_R-1}\alpha_{j1}h_j}[A]_{l_R-1,1}[A]_{l_R-1,0}^{-1}\cdots[A]_{11}[A]_{10}^{-1}\{\tilde{S}\}_{10} -$$

$$-e^{\sum_{j=l_P}^{l_R-1}\alpha_{j1}h_j}[A]_{l_R-1,1}[A]_{l_R-1,0}^{-1}\cdots[A]_{l_P1}[A]_{l_P0}^{-1}\{\tilde{S}\}^P$$

Putting

$$[H]=\begin{bmatrix}[H]_{11} & [H]_{12}\\ [H]_{21} & [H]_{22}\end{bmatrix}=[A]_{l_R-1,1}[A]_{l_R-1,0}^{-1}\cdots[A]_{l_P1}[A]_{l_P0}^{-1} \tag{26}$$

equation (22) yields

$$\{\tilde{u}\}_{l_R0} = -e^{\sum_{j=l_P}^{l_R-1}\alpha_{j1}h_j}([G]_{11}([R][S]^{-1}[T]_{21}-[T]_{11})^{-1}([F]_{12}-[R][S]^{-1}[F]_{22})+[H]_{12})\{\tilde{p}\} \tag{27}$$

(3) When $l_R=l_P$

$$\{\tilde{u}\}_{l_R0} = -[G]_{11}([R][S]^{-1}[T]_{21}-[T]_{11})^{-1}([F]_{12}-[R][S]^{-1}[F]_{22})\{\tilde{p}\} \tag{28}$$

Comparing equations (25), (27) and (28) with (4), result in that

$$\left[\tilde{Q}(\beta,\gamma)\right]=-e^{-\sum_{j=l_R}^{l_P-1}\alpha_{j1}h_j}[G]_{11}([R][S]^{-1}[T]_{21}-[T]_{11})^{-1}([F]_{12}-[R][S]^{-1}[F]_{22}) \quad (l_R<l_P) \quad (29)$$

$$\left[\tilde{Q}(\beta,\gamma)\right]=-e^{\sum_{j=l_P}^{l_R-1}\alpha_{j1}h_j}([G]_{11}([R][S]^{-1}[T]_{21}-[T]_{11})^{-1}([F]_{12}-[R][S]^{-1}[F]_{22})+[H]_{12}) \quad (l_R>l_P) \quad (30)$$

$$\left[\tilde{Q}(\beta,\gamma)\right]=-[G]_{11}([R][S]^{-1}[T]_{21}-[T]_{11})^{-1}([F]_{12}-[R][S]^{-1}[F]_{22}) \quad (l_R=l_P) \quad (31)$$

4 Some properties of $[\tilde{Q}(\beta,\gamma)]$

It is worth noting some properties of $[\tilde{Q}(\beta,\gamma)]$ that lead to efficiencies in the calculation. These are

(1) $\tilde{Q}_{13}(\beta,\gamma)$, $\tilde{Q}_{31}(\beta,\gamma)$ are odd functions of β, and even functions of γ.

(2) $\tilde{Q}_{23}(\beta,\gamma)$, $\tilde{Q}_{32}(\beta,\gamma)$ are even functions of β, and odd functions of γ.

(3) $\tilde{Q}_{11}(\beta,\gamma)$, $\tilde{Q}_{22}(\beta,\gamma)$, $\tilde{Q}_{33}(\beta,\gamma)$ are even functions of β and γ.

(4) $\tilde{Q}_{12}(\beta,\gamma)$, $\tilde{Q}_{21}(\beta,\gamma)$ are odd functions of β and γ.

(5) by putting $\beta=\rho\cos(\phi),\gamma=\rho\sin(\phi)(\therefore \rho=\sqrt{\beta^2+\gamma^2},\phi=\tan^{-1}\frac{\gamma}{\beta})$, then

$$\left[\tilde{Q}(\beta,\gamma)\right]=\begin{bmatrix}\sin\phi & \cos\phi & 0\\ -\cos\phi & \sin\phi & 0\\ 0 & 0 & 1\end{bmatrix}\left[\tilde{Q}(0,\rho)\right]\begin{bmatrix}\sin\phi & -\cos\phi & 0\\ \cos\phi & \sin\phi & 0\\ 0 & 0 & 1\end{bmatrix} \quad (32)$$

Because $\tilde{Q}_{13}(0,\rho)=\tilde{Q}_{31}(0,\rho)=\tilde{Q}_{12}(0,\rho)=\tilde{Q}_{21}(,\rho)\equiv 0$, equation (32) becomes

$$\left.\begin{aligned}
&\tilde{Q}_{13}(\beta,\gamma)=\tilde{Q}_{23}(0,\rho)\cos\phi\\
&\tilde{Q}_{23}(\beta,\gamma)=\tilde{Q}_{23}(0,\rho)\sin\phi\\
&\tilde{Q}_{33}(\beta,\gamma)=\tilde{Q}_{33}(0,\rho)\\
&\tilde{Q}_{31}(\beta,\gamma)=\tilde{Q}_{32}(0,\rho)\cos\phi\\
&\tilde{Q}_{32}(\beta,\gamma)=\tilde{Q}_{32}(0,\rho)\sin\phi\\
&\tilde{Q}_{11}(\beta,\gamma)=\tilde{Q}_{11}(0,\rho)\sin^2\phi+\tilde{Q}_{22}(0,\rho)\cos^2\phi\\
&\tilde{Q}_{22}(\beta,\gamma)=\tilde{Q}_{11}(0,\rho)\cos^2\phi+\tilde{Q}_{22}(0,\rho)\sin^2\phi\\
&\tilde{Q}_{12}(\beta,\gamma)=\tilde{Q}_{21}(\beta,\gamma)=(\tilde{Q}_{22}(0,\rho)-\tilde{Q}_{11}(0,\rho))\sin\phi\cos\phi
\end{aligned}\right\} \quad (33)$$

The fifth property is very useful, because it reduces the calculation of matrix $[\tilde{Q}]$ from a plane to an axis. On the other hand, from equations (29) to (31) in order to calculate $[\tilde{Q}]$ it is first necessary to calculate the matrices [T], [G] and [H], while the calculations of [T], [G] and [H] require calculating the inverse of the matrices $[A]_{j0}$ (j=1,2,...,n). When $\beta = 0$, from the Appendix one can see that there are many zero elements in the matrices $[A]_{j0}$, resulting in the fact that the inverse of $[A]_{j0}$ can be easily expressed analytically (omitted in this paper). As for the calculation of the inverse matrix in equations (29-31), it also can be easily expressed analytically because the matrix to be inverted is of order 3.

(6) If the Fourier transformed dynamic flexibility matrix of l_R to l_P is denoted by $[\tilde{Q}(\beta,\gamma)]$, and that of l_P to l_R by $[\tilde{\delta}(\beta,\gamma)]$, from the Betti reciprocity theorem and the axisymmetry of the problem, it can be shown that

$$\begin{bmatrix} \tilde{Q}_{11} & \tilde{Q}_{12} & \tilde{Q}_{13} \\ \tilde{Q}_{21} & \tilde{Q}_{22} & \tilde{Q}_{23} \\ \tilde{Q}_{31} & \tilde{Q}_{32} & \tilde{Q}_{33} \end{bmatrix} = \begin{bmatrix} \tilde{\delta}_{11} & \tilde{\delta}_{21} & -\tilde{\delta}_{31} \\ \tilde{\delta}_{12} & \tilde{\delta}_{22} & -\tilde{\delta}_{32} \\ -\tilde{\delta}_{13} & -\tilde{\delta}_{23} & \tilde{\delta}_{33} \end{bmatrix} \tag{34}$$

This property can be used to avoid numerical difficulties in the calculation of the Fourier transformed dynamic flexibility matrix of l_R to l_P when $l_R>l_P$. Examination of equations (29) and (31) and the Appendix shows that, when $l_R \le l_P$, no terms involve exponents of which the real parts are larger than zero, resulting in that no numerical difficulties are encountered for large layer thickness. However, when $l_R>l_P$, due to the item of $e^{\sum_{j=l_P}^{l_R-1}\alpha_{j1}h_j}$ in equation (30), this formula is inappropriate for numerical calculation. In this case, one may calculate the Fourier transformed dynamic flexibility matrix of l_P to l_R instead, and get the flexibility matrix of l_R to l_P through equation (34).

If l_R=l_P, from equation (34) result in

$$\left.\begin{aligned} \tilde{Q}_{12}(\beta,\gamma) &= \tilde{Q}_{21}(\beta,\gamma) \\ \tilde{Q}_{13}(\beta,\gamma) &= -\tilde{Q}_{31}(\beta,\gamma) \\ \tilde{Q}_{23}(\beta,\gamma) &= -\tilde{Q}_{32}(\beta,\gamma) \end{aligned}\right\} \tag{35}$$

5. Fourier transformed moving dynamic flexibility matrix of l_R to l_P

Now suppose that, in the top side of l_Pth layer, the harmonic load distributions $p_x(x,y)e^{i\Omega t}, p_y(x,y)e^{i\Omega t}, p_z(x,y)e^{i\Omega t}$ act in x, y, z directions respectively, but all move in x direction at speed c. Then the Navier's equation for the ground is

$$\left.\begin{aligned}(\lambda+\mu)\tfrac{\partial\Delta}{\partial x}+\mu\nabla^2 u=\rho\tfrac{\partial^2 u}{\partial t^2}-\delta(z-z_P)p_x(x-ct,y)e^{i\Omega t}\\(\lambda+\mu)\tfrac{\partial\Delta}{\partial y}+\mu\nabla^2 \upsilon=\rho\tfrac{\partial^2 \upsilon}{\partial t^2}-\delta(z-z_P)p_y(x-ct,y)e^{i\Omega t}\\(\lambda+\mu)\tfrac{\partial\Delta}{\partial z}+\mu\nabla^2 w=\rho\tfrac{\partial^2 w}{\partial t^2}-\delta(z-z_P)p_z(x-ct,y)e^{i\Omega t}\end{aligned}\right\} \tag{36}$$

where z_P is the depth of the top side of the l_Pth layer, and $\delta(.)$ is the Dirac-δ function. The Fourier transform of equation (36) is

$$\left.\begin{aligned}(\lambda+\mu)i\beta\overline{\Delta}+\mu[\tfrac{d^2\overline{u}}{dz^2}-(\beta^2+\gamma^2)\overline{u}]=\rho\tfrac{\partial^2\overline{u}}{\partial t^2}-\delta(z-z_P)\widetilde{p}_x(\beta,\gamma)e^{i(\Omega-\beta c)t}\\(\lambda+\mu)i\gamma\overline{\Delta}+\mu[\tfrac{d^2\overline{\upsilon}}{dz^2}-(\beta^2+\gamma^2)\overline{\upsilon}]=\rho\tfrac{\partial^2\overline{\upsilon}}{\partial t^2}-\delta(z-z_P)\widetilde{p}_y(\beta,\gamma)e^{i(\Omega-\beta c)t}\\(\lambda+\mu)\tfrac{d\overline{\Delta}}{dz}+\mu[\tfrac{d^2\overline{w}}{dz^2}-(\beta^2+\gamma^2)\overline{w}]=\rho\tfrac{\partial^2\overline{w}}{\partial t^2}-\delta(z-z_P)\widetilde{p}_z(\beta,\gamma)e^{i(\Omega-\beta c)t}\end{aligned}\right\} \tag{37}$$

where $\widetilde{p}_x(\beta,\gamma),\widetilde{p}_y(\beta,\gamma),\widetilde{p}_z(\beta,\gamma)$ are Fourier transforms of $p_x(x,y),p_y(x,y),p_z(x,y)$. Now the steady state solution to equation (37) may be written as

$$\left.\begin{aligned}\overline{\Delta}&=\widetilde{\Delta}e^{i(\Omega-\beta c)t}\\\overline{u}&=\widetilde{u}e^{i(\Omega-\beta c)t}\\\overline{\upsilon}&=\widetilde{\upsilon}e^{i(\Omega-\beta c)t}\\\overline{w}&=\widetilde{w}e^{i(\Omega-\beta c)t}\end{aligned}\right\} \tag{38}$$

Equation (38) means that, if $u^*(x,y,z)$ is the inverse Fourier transform of $\widetilde{u}(\beta,\gamma,z)$, the actual longitudinal displacement of point (x,y,z) in the ground is given by $u(x,y,z,t)=u^*(x-ct,y,z)e^{i\Omega t}$.

With the substitution of equation (38) into equation (37) yeilds,

$$\left.\begin{aligned}(\lambda+\mu)i\beta\widetilde{\Delta}+\mu[\tfrac{d^2\widetilde{u}}{dz^2}-(\beta^2+\gamma^2)\widetilde{u}]=-\rho(\Omega-\beta c)^2\widetilde{u}-\delta(z-z_P)\widetilde{p}_x(\beta,\gamma)\\(\lambda+\mu)i\gamma\widetilde{\Delta}+\mu[\tfrac{d^2\widetilde{\upsilon}}{dz^2}-(\beta^2+\gamma^2)\widetilde{\upsilon}]=-\rho(\Omega-\beta c)^2\widetilde{\upsilon}-\delta(z-z_P)\widetilde{p}_y(\beta,\gamma)\\(\lambda+\mu)\tfrac{d\widetilde{\Delta}}{dz}+\mu[\tfrac{d^2\widetilde{w}}{dz^2}-(\beta^2+\gamma^2)\widetilde{w}]=-\rho(\Omega-\beta c)^2\widetilde{w}-\delta(z-z_P)\widetilde{p}_z(\beta,\gamma)\end{aligned}\right\} \tag{39}$$

This equation is the same as equation (9) if put

$$\omega=\Omega-\beta c \tag{40}$$

therefore for the top side of l_Rth layer comes

$$\begin{Bmatrix}\widetilde{u}_{l_R0}(\beta,\gamma)\\\widetilde{\upsilon}_{l_R0}(\beta,\gamma)\\\widetilde{w}_{l_R0}(\beta,\gamma)\end{Bmatrix}=[\widetilde{Q}(\beta,\gamma)]\begin{Bmatrix}\widetilde{p}_x(\beta,\gamma)\\\widetilde{p}_y(\beta,\gamma)\\\widetilde{p}_z(\beta,\gamma)\end{Bmatrix} \tag{41}$$

and from equation (38) the time varying Fourier transformed displacements on the top side of the l_Rth layer are obtained by mutiplying the factor $e^{i(\Omega-\beta c)t}$.

The matrix $[\widetilde{Q}(\beta,\gamma)]$ is called *Fourier transfromed along x-axle moving dynamic flexibility matrix of l_R to l_P* (meaning that, the unit harmonic load moving along x-axle on the top side of

l_Pth layer and the displacements are for the top side of l_Rth layer), or simply, *Fourier transformed moving dynamic flexibility matrix.* The caulation of this matrix is exactly the same as described in section 3 if put $\omega = \Omega - \beta c$.

This matrix may be denoted by $[\tilde{Q}(\beta,\gamma,\Omega-\beta c)]$ to emphasise its dependence on $\omega = \Omega - \beta c$. It can be shown that,

(1) by putting $\beta = \rho\cos(\phi), \gamma = \rho\sin(\phi) (\therefore \rho = \sqrt{\beta^2+\gamma^2}, \phi = \tan^{-1}\frac{\gamma}{\beta})$, then

$$[\tilde{Q}(\beta,\gamma,\Omega-\beta c)] = \begin{bmatrix} \sin\phi & \cos\phi & 0 \\ -\cos\phi & \sin\phi & 0 \\ 0 & 0 & 1 \end{bmatrix} [\tilde{Q}(0,\rho,\Omega-\beta c)] \begin{bmatrix} \sin\phi & -\cos\phi & 0 \\ \cos\phi & \sin\phi & 0 \\ 0 & 0 & 1 \end{bmatrix} \tag{42}$$

(2) If the matrix of l_R to l_P is denoted by $[\tilde{Q}(\beta,\gamma,\Omega-\beta c)]$, and that of l_P to l_R by $[\tilde{\delta}(\beta,\gamma,\Omega-\beta c)]$, it can be shown that

$$\begin{bmatrix} \tilde{Q}_{11} & \tilde{Q}_{12} & \tilde{Q}_{13} \\ \tilde{Q}_{21} & \tilde{Q}_{22} & \tilde{Q}_{23} \\ \tilde{Q}_{31} & \tilde{Q}_{32} & \tilde{Q}_{33} \end{bmatrix}_{(\beta,\gamma,\Omega-\beta c)} = \begin{bmatrix} \tilde{\delta}_{11} & \tilde{\delta}_{21} & -\tilde{\delta}_{31} \\ \tilde{\delta}_{12} & \tilde{\delta}_{22} & -\tilde{\delta}_{32} \\ -\tilde{\delta}_{13} & -\tilde{\delta}_{23} & \tilde{\delta}_{33} \end{bmatrix}_{(\beta,\gamma,\Omega-\beta c)} \tag{43}$$

where the item in the round brackets indicates that each elememt of the matrices is a function of β,γ and $\Omega-\beta c$.

(3) Reciprocity relations

Suppose at time t=0 a vertical (in z direction) unit harmonic load moving in the positive x-direction acts at the point (r,s) on the top side of l_Pth layer, i.e. $p_x = 0, p_y = 0, p_z = \delta(x-r, y-s)$, and $\tilde{p}_x = 0, \tilde{p}_y = 0, \tilde{p}_z = e^{-i(\beta r+\gamma s)}$, then the longitudinal (in x-direction) displacement of point (p,q) on the top side of l_Rth layer comes from equations (38) and (41) as follows

$$u_{l_R0}(p,q,t) = \frac{1}{4\pi^2}\int_{-\infty}^{\infty}\int_{-\infty}^{\infty}\tilde{Q}_{13}(\beta,\gamma,\Omega-\beta c)e^{i(\Omega-\beta c)t}e^{i\beta(p-r)}e^{i\gamma(q-s)}d\beta d\gamma \tag{a}$$

Now let the source-observer configuration be interchanged, i.e. at time t=0 a longitidinal unit harmonic load moving in the negative x-direction acts at the point (p,q) on the top side of the l_Rth layer, i.e. $p_x = \delta(x-p, y-q), p_y = 0, p_z = 0$, and $\tilde{p}_x = e^{-i(\beta p+\gamma q)}, \tilde{p}_y = 0, \tilde{p}_z = 0$, then the vertical displacement of point (r,s) on the top side of l_Pth layer comes from equations (38) and (41)

$$w_{l_P0}(r,s,t) = \frac{1}{4\pi^2}\int_{-\infty}^{\infty}\int_{-\infty}^{\infty}\tilde{\delta}_{31}(\beta,\gamma,\Omega+\beta c)e^{i(\Omega+\beta c)t}e^{i\beta(r-p)}e^{i\gamma(s-q)}d\beta d\gamma \tag{b}$$

From equation (43), (b) becomes

$$w_{l_p0}(r,s,t) = -\frac{1}{4\pi^2}\int_{-\infty}^{\infty}\int_{-\infty}^{\infty}\tilde{Q}_{13}(\beta,\gamma,\Omega+\beta c)e^{i(\Omega+\beta c)t}e^{i\beta(r-p)}e^{i\gamma(s-q)}d\beta d\gamma$$

which, due to $\tilde{Q}_{13}(-\beta,-\gamma,\Omega-\beta c) = -\tilde{Q}_{13}(\beta,\gamma,\Omega-\beta c)$, can be written as

$$w_{l_p0}(r,s,t) = \frac{1}{4\pi^2}\int_{-\infty}^{\infty}\int_{-\infty}^{\infty}\tilde{Q}_{13}(\beta,\gamma,\Omega-\beta c)e^{i(\Omega-\beta c)t}e^{i\beta(p-r)}e^{i\gamma(q-s)}d\beta d\gamma \qquad \text{(c)}$$

Equations (a) and (b) show that $u_{l_R0}(p,q,t) = w_{l_p0}(r,s,t)$. It can be further conclude that:

The displacement of point A in direction 1 due to a unit harmonic load acting in direction 2 and moving at speed *c* along a line parallel to the ground surface and passing through point B (called line B, at *t*=0, the load acts at point B), is equal to the displacement of point B in direction 2 due to a unit harmonic load of same frequency acting in direction 1 and moving inversely at speed *c* along line A which passes point A and is parallel to line B (at *t*=0, the load acts at point A).

Barros and Luco (1994, section 4.3) have noticed the reciprocity relations for a special case, i.e. *r=p, s=q*, through numerical test other than a proof.

6 Example calculations for comparison with the previous work

To validate the theory developed in this paper, several examples used by other researchers have been calculated using the dynamic flexibility matrix approach. The first example is a ground comprising of one layer of 7m which overlies a rigid foundation (D.V. Jones and M. Petyt 1997) subject to a unit rectangular harmonic load of 64 Hz on the ground surface. The parameters for the gound are listed in Table 1. Now $p_x = 0$, $p_y = 0$ for all points and $p_z = P_0/4ab$ when $-a \le x \le a$ and $-b \le y \le b$, where a=b=0.3m and P_0=1N, and $p_z = 0$ at other points. This gives $\tilde{p}_x = 0, \tilde{p}_y = 0, \tilde{p}_z = \frac{\sin\beta a}{\beta a}\frac{\sin\gamma b}{\gamma b}P_0$, and substituting them into equation (4) yields,

$$\left.\begin{aligned}\tilde{u}_{l_R0}(\beta,\gamma) &= \tilde{Q}_{13}(\beta,\gamma)\tfrac{\sin\beta a}{\beta a}\tfrac{\sin\gamma b}{\gamma b}P_0\\ \tilde{\upsilon}_{l_R0}(\beta,\gamma) &= \tilde{Q}_{23}(\beta,\gamma)\tfrac{\sin\beta a}{\beta a}\tfrac{\sin\gamma b}{\gamma b}P_0\\ \tilde{w}_{l_R0}(\beta,\gamma) &= \tilde{Q}_{33}(\beta,\gamma)\tfrac{\sin\beta a}{\beta a}\tfrac{\sin\gamma b}{\gamma b}P_0\end{aligned}\right\} \qquad (42)$$

Figure 1 shows the amplitude of Fourier transformed vertical displacement of the ground surface, which, if divided by $4\pi^2$, is exact the same as that obtained by D.V. Jones and M. Petyt (Jones and Petyt 1997, Figure 3) by dividing the 7m layer into 7 sublayers. Figures 2 and 3 show the amplitude of the Fourier transformed vertical displacement and the amplitude of the actual longintudinal (in *x*-direction) displacement of the horizontal plane of 3m depth in the ground. As to the amplitude of the actual longitudinal displacement of the ground surface, this is shown in Figure 4.

TABLE 1

The parameters for the ground

layer	depth (m)	Young's modulus (Mpa)	Possion ratio	Density (kg/m^3)	Loss factor	P-wave speed (m/s)	S-wave speed (m/s)	Rayleigh-wave speed (m/s)
1	7	269	0.257	1550	0.1	459.43	262.74	242.01
half	space	1076	0.257	2000	0.1			

For the second example, instead of the rigid foundation, the same ground layer overlies an elastic half space (D.V. Jones and M. Petyt 1998) subject to the same rectangular harmonic load on the ground surface. The parameters for the half space are listed in Table 1. Figure 5 shows the amplitude of vertical displacements along *y*-axis on the ground surface, which is exact the same as that obtained by D.V. Jones and M. Petyt (Jones and Petyt 1998, Figure 5). Figure 6 shows the overall vertical displacements of the ground surface.

The third example comes from the paper by F.C.P. de Barros and J.E.Luco (1994). The ground is a uniform half space with Young's modulus 5000Mpa, Possion ratio 0.25, density 2000kg/m^3 (P-wave speed=1732m/s, S-wave speed=1000m/s), loss factor 0.002, subject to a unit load of 0Hz acting downward on the ground surface and moving along the *x*-axis at speed *c*=700m/s. Figures 7 and 8 show the vertical and longitudinal displacemets on a horizontal plane of 10m depth, from which the curve of the dimensionless vertical displacement(=real displacement times 2 10^{10}) against dimensionless time(=real time multiplied by 100, the range of real time =range of distance in figure 7 divided by load speed) and the curve of dimesionless longitudinal displacement *versus* dimesionless time of the point (0,0,10), can be obtained as shown in Figures 9 and 10, which are very close to that obtained by F.C.P. de Barros and J.E. Luco (Figure 6 in their paper).

7 Conclusions

In this paper, a more efficient and analytical method is proposed to calculate the Fourier transformed stationary dynamic flexibility matrix which is constructed from the steady state displacements due to unit stationary harmonic load, and the Fourier transformed moving dynamic flexibility matrix comprising of the steady state displacements due to unit harmonic load moving uniformly along a line parallel to the ground surface. The source and obsever may be located on the ground surface or at any depth in the ground. Example calculations are made to compare with other methods and to validate the present approach. These flexibility matrices will lead to significant advances in the investigation of a viariety of radiation, scattering and interaction problems associated with stationary and moving disturbances in a layered ground, such as surface trains and underground trains. The reciprocity relations which are well known in the stationary case are extended to the moving case: The displacement of point A in direction 1 due to a unit harmonic load acting in direction 2 and moving at speed c along a line parallel to the ground surface and passing through point B (called line B, at t=0, the load acts at point B), is equal to the displacement of point B in direction 2 due to a unit harmonic load of the same frequency acting in direction 1 and moving inversely at speed c along line A which passes point A and is parallel to line B (at t=0, the load acts at point A).

REFERENCES

Apsel , R. and Luco, J. (1983). On the Green's functions for a layered half-space. Part II, *Bulletin of the Seismological Society of America* **73**: 931-951.

Barros, F. and Luco, J. (1994). Response of a layered viscoelasic half-space to a moving point load, *Wave Motion* **19**: 189-210.

Jones, D.V. and Petyt, M. (1997). Ground vibration in the vicinity of a rectangular load acting on a viscoelastic layer over a rigid foundation, *Journal of Sound and Vibration* **203**(2): 307-319.

Jones, D.V. and Petyt, M. (1998). Ground vibration due to a rectangular harmonic load. *Journal of Sound and Vibration* **212**(1): 61-74.

Haskell, N.(1953). The dispersion of surface waves on multilayered medium, *Bulletin of the Seismological Society of America* **73**: 17-43

Kausel, E. (1986). Wave propagation in anisotropic layered media, *International Journal for Numerical Methods in Engineering* **23**: 1567-1578.

Kausel, E. and Peek, R. (1982). Dynamic loads in the interior of a layered stratum: an explicit solution, *Bulletin of the Seismological Society of America* **72**(5): 1469-1481.

Kausel, E. and Roesset, J. (1981). Stiffness matrices for a layered soils, *Bulletin of the Seismological Society of America* **71**(6): 1743-1761.

Luco, J. and Apsel, R. (1983). On the Green's functions for a layered half space. Part I, *Bulletin of the Seismological Society of America* **4**: 909-929.

Lysmer, J. and Waas, G. (1972). Shear waves in plane infinite structure, *Journal of the Engineering Mechanics Division, Proceedings of the ASCE* **98** (EM1): 85-105.

Tassoulas, J. and Kausel, E. (1983). Elements for the numerical analysis of wave motion in layered strata, *International Journal for Numerical Methods in Engineering* **19**(7): 1005-1032.

Thomson, W. (1950). Transmission of elastic waves though a stratified solid medium, *Journal of Applied Physics* **21**: 89-93.

Waas, G. (1972). Linear two-dimensional analysis of soil dynamic problems in semiinfinite layer medium, *PhD thesis*, Department of Civil Engineering, University of California, Berkeley.

Wolf, J. (1985). *Dynamics soil-structure interaction*, Prentice-Hall, Englewood Gliffs, New Jersey.

APPENDIX

Putting

$$\zeta_{j1}=\omega/c_{j1},\zeta_{j2}=\omega/c_{j2}$$

$$\alpha_{j1}=\sqrt{\beta^2+\gamma^2-\zeta_{j1}^2},\alpha_{j2}=\sqrt{\beta^2+\gamma^2-\zeta_{j2}^2}$$

then

A1 When $\beta=0$, and $\omega\neq0$

A1.1 Matrix $[A]_{j0}=(a_{kl})$ $(k,l=1,2,..6;j=1,2,..,n)$

$$a_{12}=1,a_{15}=1,a_{23}=1,a_{26}=1,$$

$$a_{21}=-i\gamma/\zeta_{j1}^2,a_{24}=a_{21}$$

$$a_{31}=-\alpha_{j1}/\zeta_{j1}^2,a_{33}=-i\gamma/\alpha_{j2},a_{34}=-a_{31},a_{36}=-a_{33}$$

$$a_{42}=\alpha_{j2}\mu_j,a_{45}=-a_{42}$$

$$a_{51}=-2i\mu_j\alpha_{j1}\gamma/\zeta_{j1}^2,a_{53}=\mu_j(\gamma^2/\alpha_{j2}+\alpha_{j2}),a_{54}=-a_{51},a_{56}=-a_{53}$$

$$a_{61}=-\mu_j(\zeta_{j2}^2+2\alpha_{j2}^2)/\zeta_{j1}^2,a_{63}=-2i\mu_j\gamma,a_{64}=a_{61},a_{66}=a_{63}$$

other a's are zero.

A1.2 Matrix $[A]_{j1}$ $(j=1,2,..,n)$

$$[A]_{j1}=[A]_{j0}[D]_j$$

where $[D]_j$ is a diagonal matrix with the elements of

$$d_{11}=1,d_{22}=e^{(\alpha_{j2}-\alpha_{j1})h_j},d_{33}=d_{22},d_{44}=e^{-2\alpha_{j1}h_j}$$

$$d_{55}=e^{-(\alpha_{j1}+\alpha_{j2})h_j},d_{66}=d_{55}$$

A1.3 Matrix $[R]$ and $[S]$

$$[R]=\begin{bmatrix}0 & 1 & 0\\ -\frac{i\gamma}{\zeta_{n+1,1}^2} & 0 & 1\\ \frac{\alpha_{n+1,1}}{\zeta_{n+1,1}^2} & 0 & \frac{i\gamma}{\alpha_{n+1,2}}\end{bmatrix}$$

$$[S]=\begin{bmatrix}0 & -\mu_{n+1}\alpha_{n+1,2} & 0\\ \frac{2i\mu_{n+1}\alpha_{n+1,1}\gamma}{\zeta_{n+1,1}^2} & 0 & -\frac{\mu_{n+1}(\gamma^2+\alpha_{n+1,2}^2)}{\alpha_{n+1,2}}\\ \lambda_{n+1}-2\mu_{n+1}\frac{\alpha_{n+1,1}^2}{\zeta_{n+1,1}^2} & 0 & -2i\mu_{n+1}\gamma\end{bmatrix}$$

A2 When $\beta = 0$, and $\omega = 0$

A2.1 Matrix $[A]_{j0} = (a_{kl})$ $(k,l=1,2,..6; j=1,2,..,n)$

$$a_{12} = 1, a_{15} = 1, a_{23} = 1, a_{26} = 1$$

$$a_{31} = (\lambda_j + 3\mu_j) / 2\alpha_{j1}\mu_j, a_{33} = -i\gamma / \alpha_{j2}, a_{34} = -a_{31}, a_{36} = -a_{33}$$

$$a_{42} = \alpha_{j2}\mu_j, a_{45} = -a_{42}$$

$$a_{51} = i\mu_j\gamma / \alpha_{j1}, a_{53} = \mu_j(\gamma^2 / \alpha_{j2} + \alpha_{j2}), a_{54} = -a_{51}, a_{56} = -a_{53}$$

$$a_{61} = \lambda_j + 2\mu_j, a_{63} = -2i\mu_j\gamma, a_{64} = a_{61}, a_{66} = a_{63}$$

other a's are zero.

A2.2 Matrix $[A]_{j1}$ $(j=1,2,..,n)$

$$[A]_{j1} = [A']_{j0}[D]_j$$

where $[D]_j$ is a diagonal matrix with the elements of

$$d_{11} = 1, d_{22} = e^{(\alpha_{j2} - \alpha_{j1})h_j}, d_{33} = d_{22}, d_{44} = e^{-2\alpha_{j1}h_j}$$

$$d_{55} = e^{-(\alpha_{j1} + \alpha_{j2})h_j}, d_{66} = d_{55}$$

and $[A']_{j0} = (a'_{kl})(k,l = 1,2,\ldots,6; j = 1,2,\ldots,n)$ are 6x6 matrices the elements of which are the same as that of $[A]_{j0}$ except for the elements in the first and fourth columns:

$$a'_{11} = 0, a'_{21} = -\tfrac{i(\lambda_j+\mu_j)\gamma h_j}{2\alpha_{j1}\mu_j}, a'_{31} = \tfrac{\lambda_j+3\mu_j}{2\alpha_{j1}\mu_j} - \tfrac{\lambda_j+\mu_j}{2\mu_j}h_j$$

$$a'_{41} = 0, a'_{51} = i\gamma[\tfrac{\mu_j}{\alpha_{j1}} - (\lambda_j + \mu_j)h_j], a'_{61} = (\lambda_j + \mu_j)(\mu_j - a_{j1}h_j)$$

$$a'_{14} = 0, a'_{24} = -a'_{21}, a'_{34} = -(\tfrac{\lambda_j+3\mu_j}{2\alpha_{j1}\mu_j} + \tfrac{\lambda_j+\mu_j}{2\mu_j}h_j)$$

$$a'_{44} = 0, a'_{54} = -i\gamma[\tfrac{\mu_j}{\alpha_{j1}} + (\lambda_j + \mu_j)h_j], a'_{64} = (\lambda_j + \mu_j)(\mu_j + a_{j1}h_j)$$

A2.3 Matrix $[R]$ and $[S]$

$$[R] = \begin{bmatrix} 0 & 1 & 0 \\ 0 & 0 & 1 \\ -\frac{\lambda_{n+1}+3\mu_{n+1}}{2\alpha_{n+1,1}\mu_{n+1}} & 0 & \frac{i\gamma}{\alpha_{n+1,2}} \end{bmatrix}$$

$$[S] = \begin{bmatrix} 0 & -\mu_{n+1}\alpha_{n+1,2} & 0 \\ -\frac{i\gamma\mu_{n+1}}{\alpha_{n+1,1}} & 0 & -\frac{\mu_{n+1}(\gamma^2+\alpha_{n+1,2}^2)}{\alpha_{n+1,2}} \\ \lambda_{n+1} + 2\mu_{n+1} & 0 & -2i\mu_{n+1}\gamma \end{bmatrix}$$

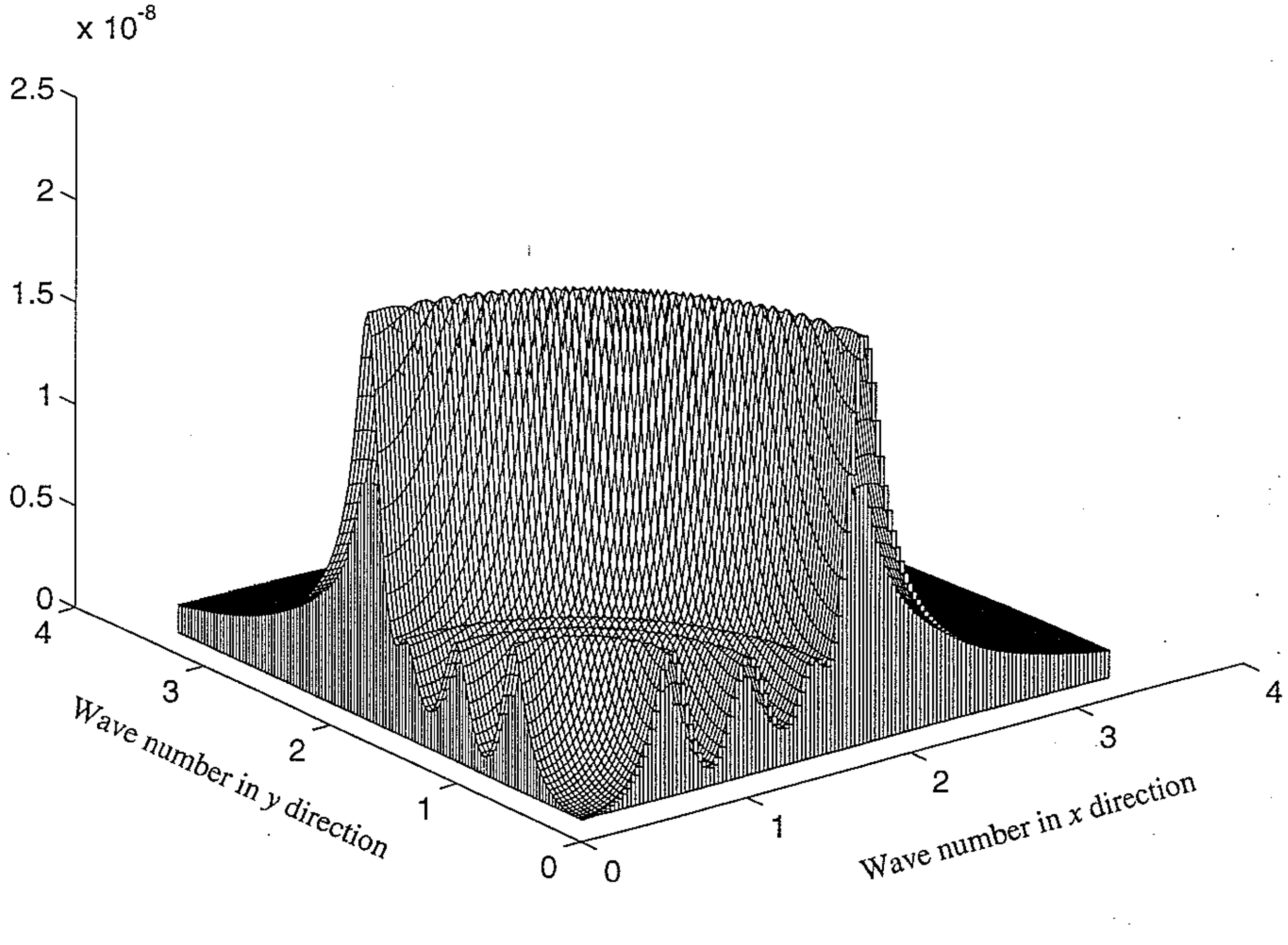

Figure 1 Amplitude of the Fourier transformed vertical displacement of the ground surface due to a surface unit rectangular harmonic load of 64Hz. The ground parameters are listed in Table 1 with a 7m layer overlying a rigid foundation.

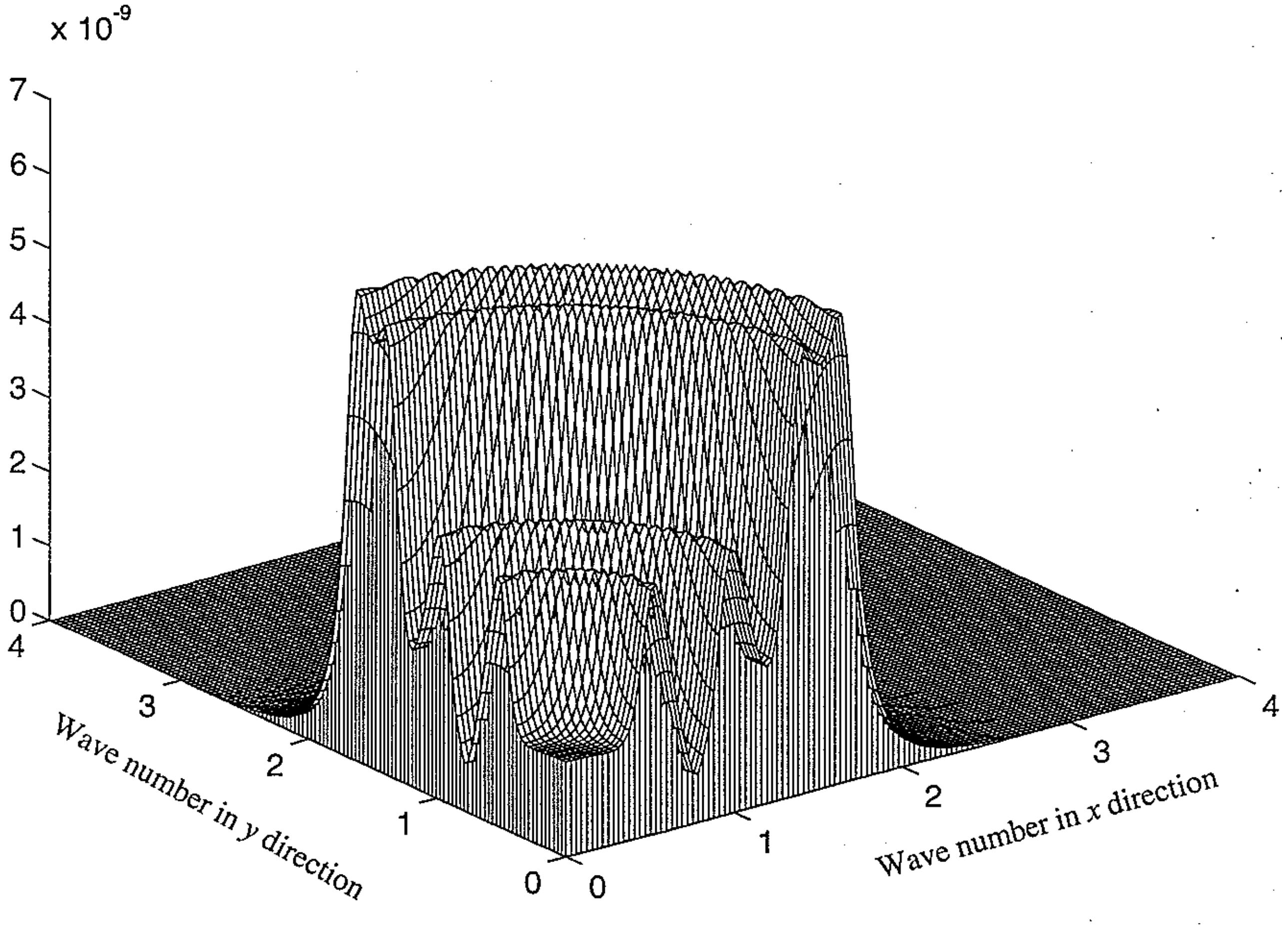

Figure 2 Amplitude of Fourier transformed vertical displacement of the horizontal plane of 3m depth in the ground due to a surface unit rectangular harmonic load of 64Hz. the ground parameters are listed in Table 1 with a 7m layer overlying a rigid foundation.

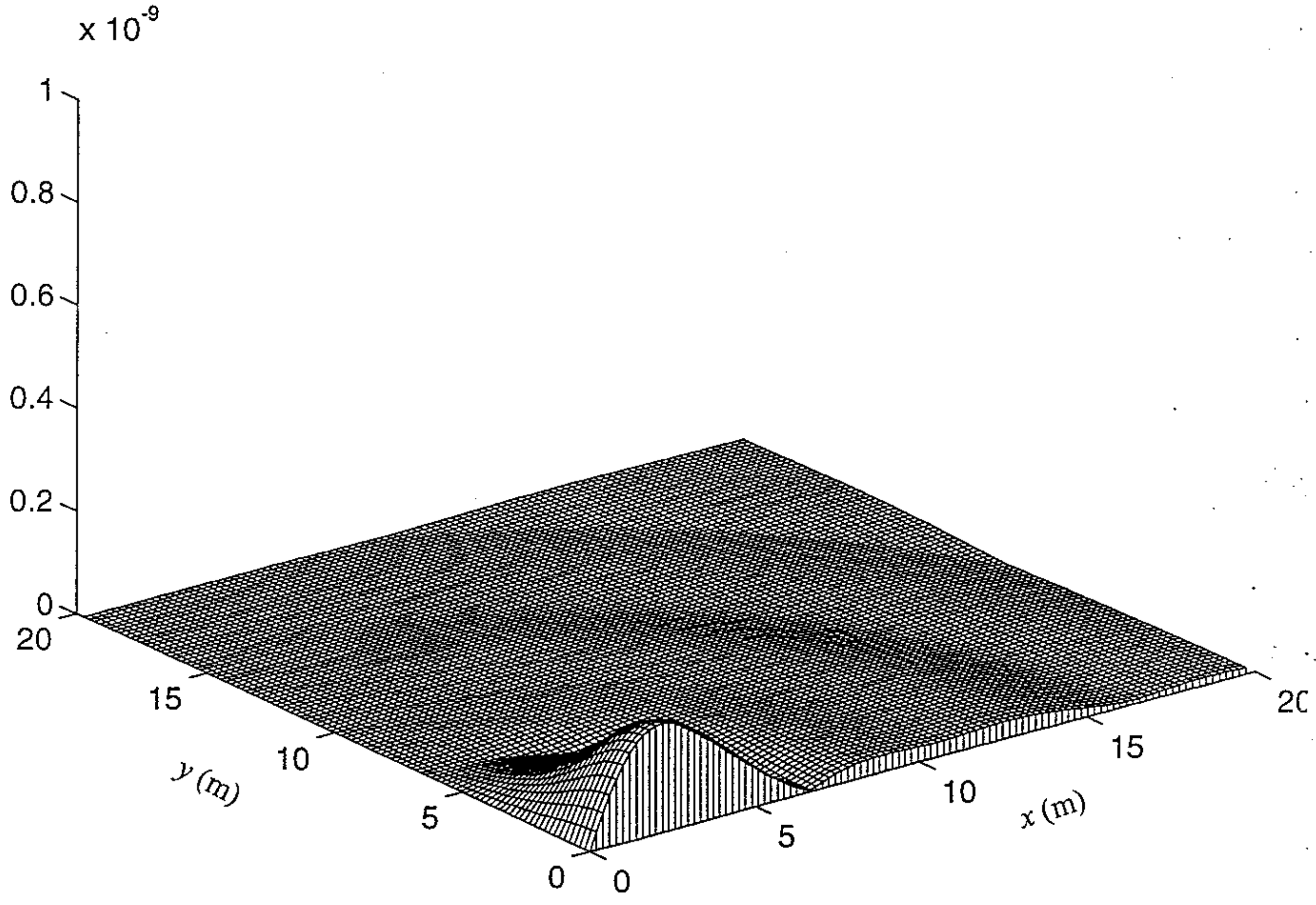

Figure 3 Amplitude of the longitudinal displacement of the horizontal plane of 3m depth in the ground due to a surface unit rectangular harmonic load of 64Hz. Ground parameters are listed in Table 1 with a 7m layer overlying a rigid foundation.

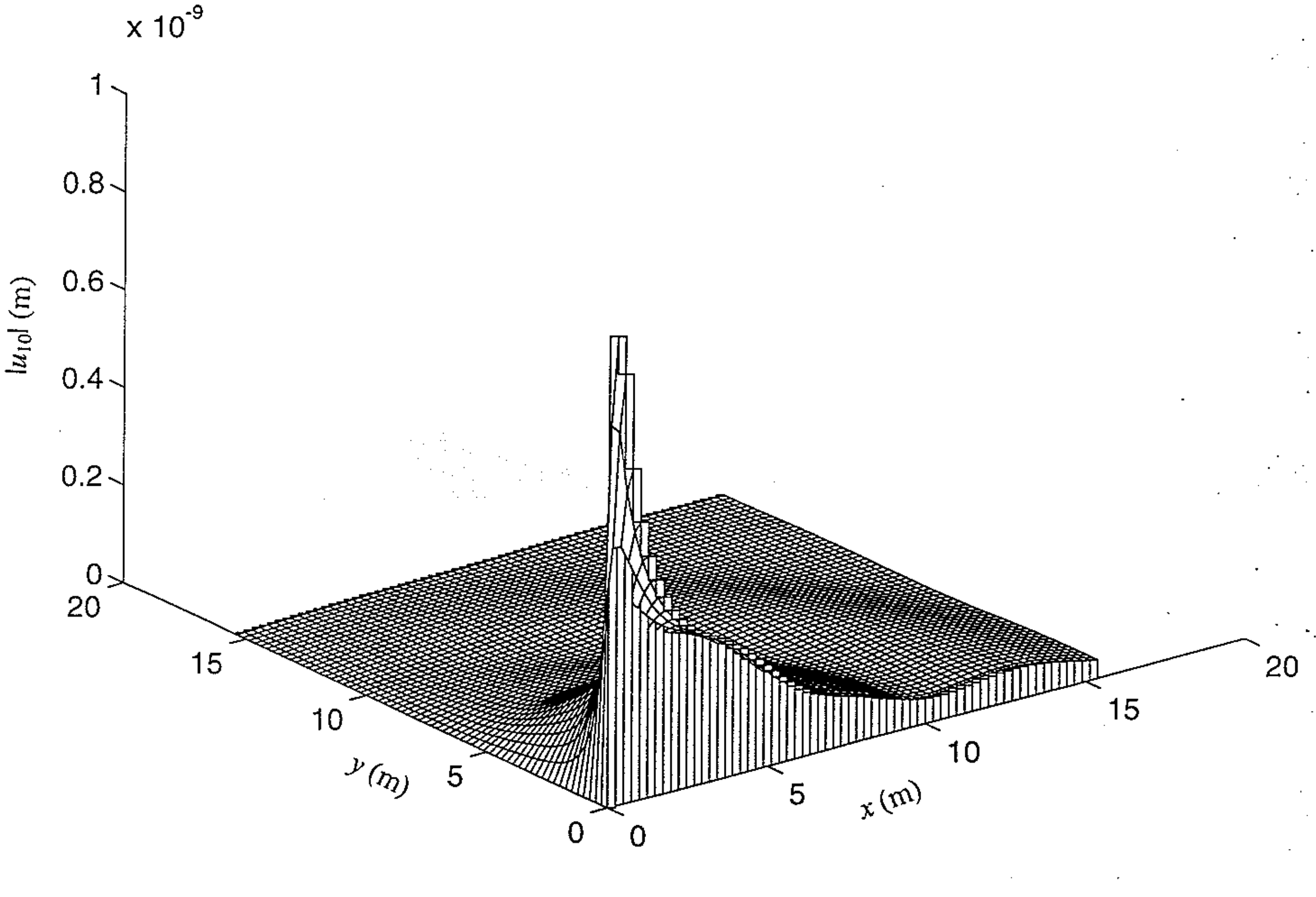

Figure 4 Amplitude of the longitudinal displacement of the ground surface due to a surface unit rectangular harmonic load of 64Hz. the ground parameters are listed in Table 1 with a 7m layer overlying a rigid foundation.

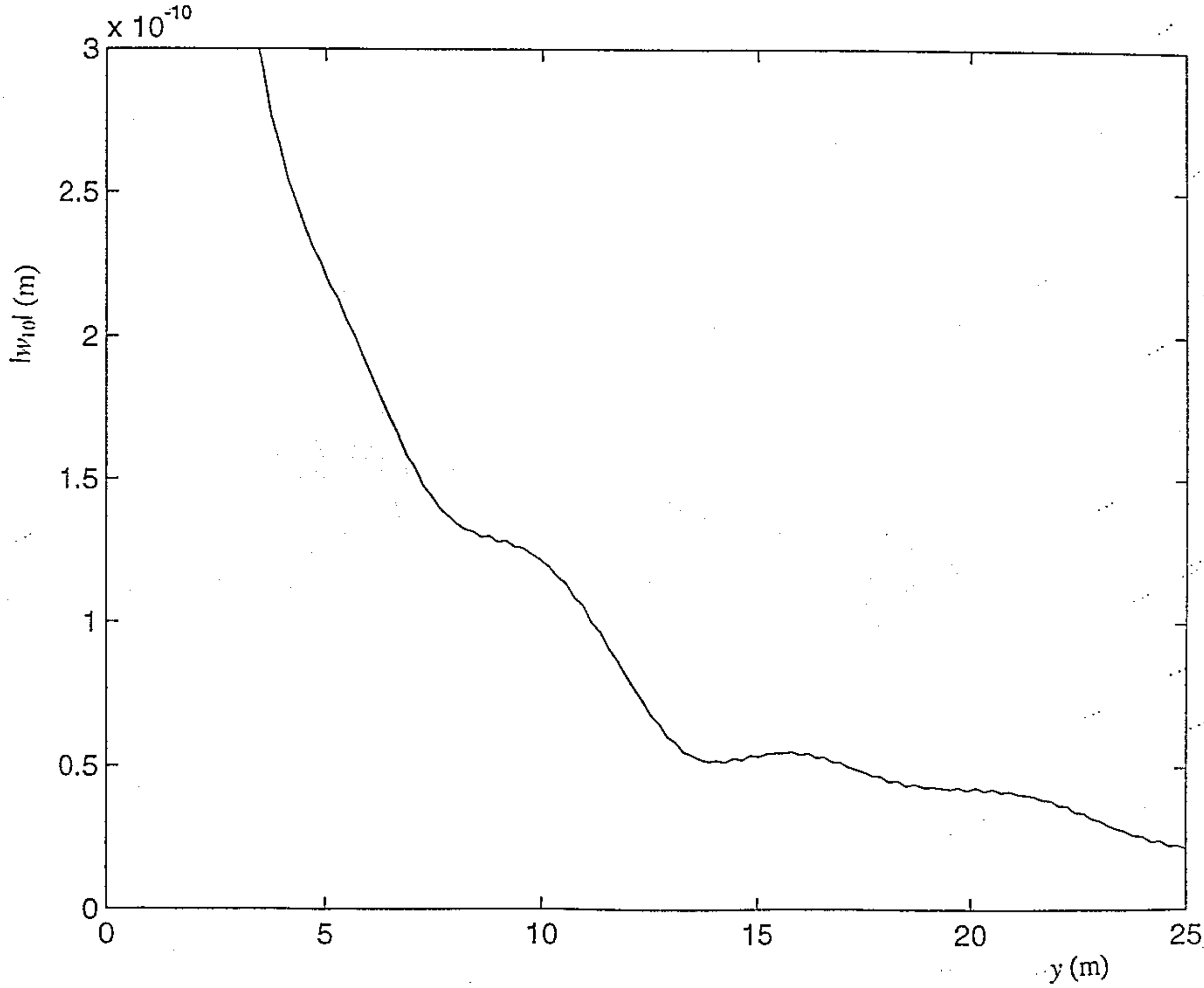

Figure 5 Amplitude of the vertical displacement along *y*-axis on the the ground surface due to a surface unit rectangular harmonic load of 64Hz. the ground parameters are listed in Table 1 with a 7m layer overlying a half space.

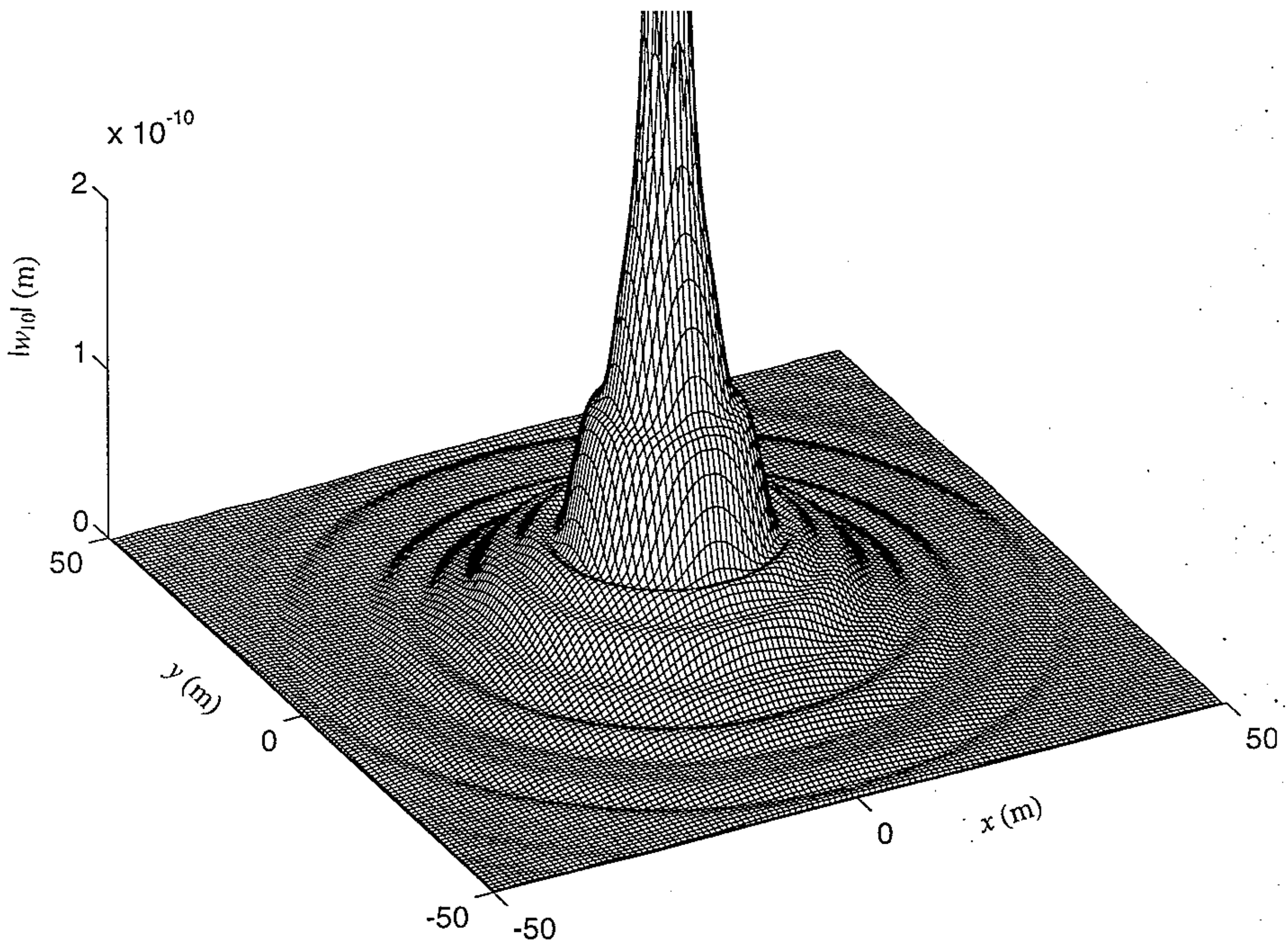

Figure 6 Amplitude of the vertical displacement of the ground surface due to a surface unit rectangular harmonic load of 64Hz. The ground parameters are listed in Table 1 with a 7m layer overlying a half space.

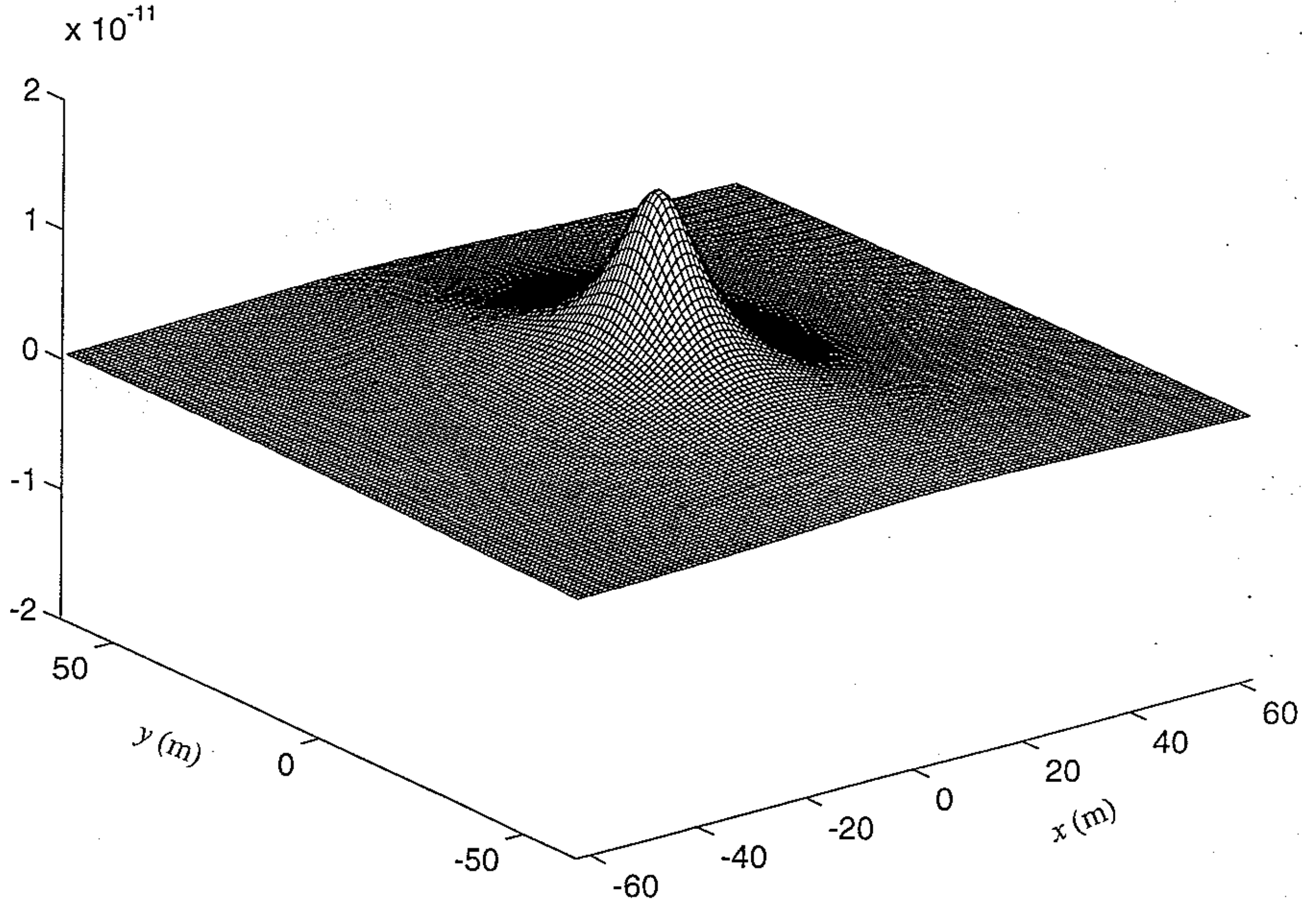

Figure 7 The vertical displacement of the horizontal plane of 10m depth in the ground due to a unit constant point load moving at speed c=700m/s along the positive x-direction over the surface of a uniform viscoelastic half-space.

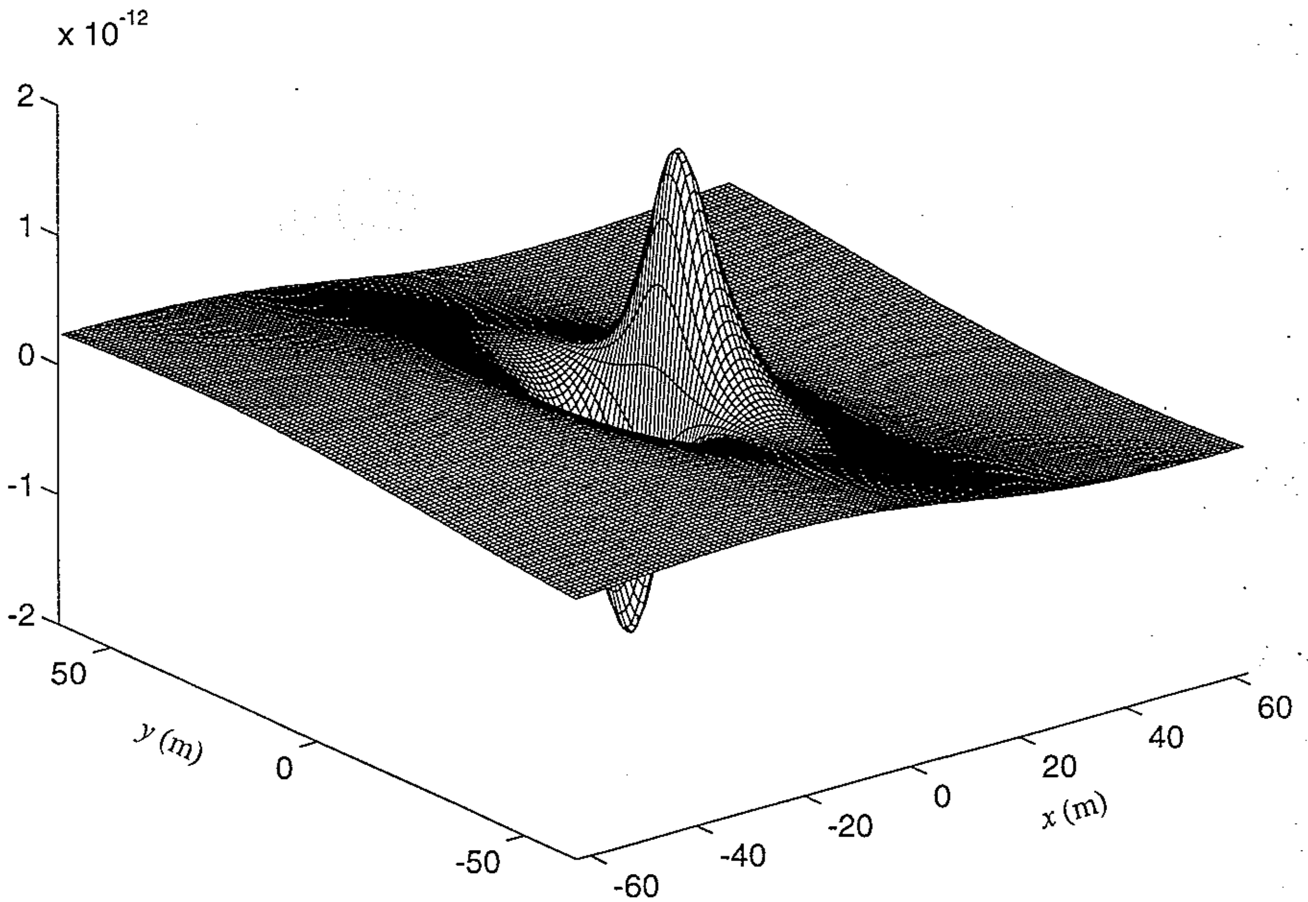

Figure 8 The longitudinal displacement of the horizontal plane of 10m depth in the ground due to a unit constant point load moving at speed c=700m/s along the positive x-direction over the surface of a uniform viscoelastic half-space.

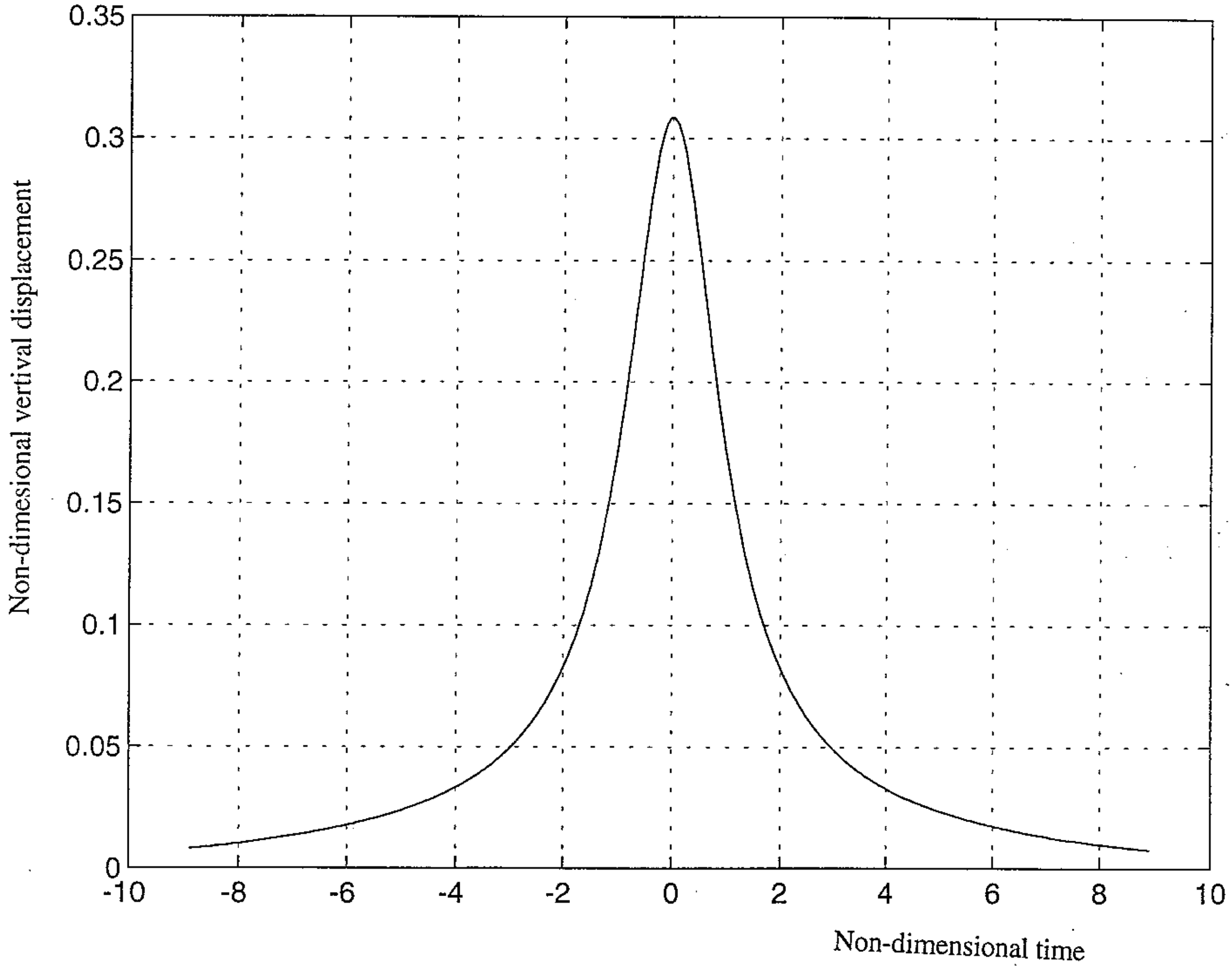

Figure 9 The non- dimensional vertical displacement of an observation point (0,0, 10m) in the ground due to a unit constant point load moving with c=700m/s along the positive x-direction over the surface of a uniform viscoelastic half-space.

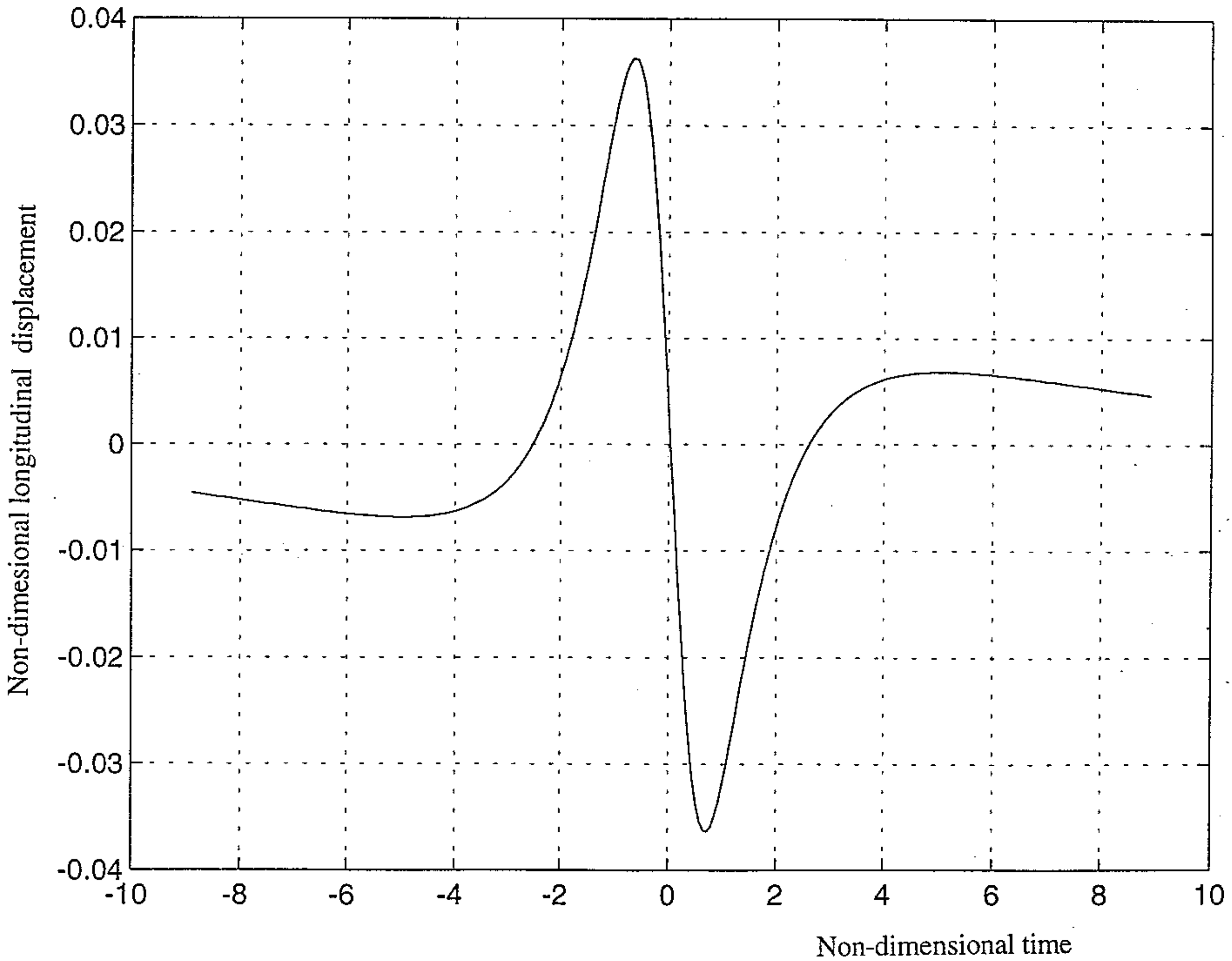

Figure 10 The non-dimensional longitudinal displacement of an observation point (0, 0, 10m) in the ground due to a unit constant point load moving at speed c=700m/s along the positive x-direction over the surface of a uniform viscoelastic half-space.